The Astrophysical Journal, 842:96 (10pp), 2017 June 20 https://doi.org/10.3847/1538-4357/aa72f4

Optical Variability of Narrow-line and Broad-line Seyfert 1 Galaxies

Suvendu Rakshit and C. S. Stalin
Indian Institute of Astrophysics, Block II, Koramangala, Bangalore-560034, India; suvenduat@gmail.com
Received 2017 January 30; revised 2017 May 10; accepted 2017 May 12; published 2017 June 19

Abstract

We studied the optical variability (OV) of a large sample of narrow-line Seyfert 1 (NLSy1) and broad-line Seyfert 1 (BLSy1) galaxies with $z < 0.8$ to investigate any differences in their OV properties. Using archival optical *V*-band light curves from the Catalina Real Time Transient Survey that span 5–9 years and modeling them using damped random walk, we estimated the amplitude of variability. We found that NLSy1 galaxies as a class show lower amplitude of variability than their broad-line counterparts. In the sample of both NLSy1 and BLSy1 galaxies, radio-loud sources are found to have higher variability amplitude than radio-quiet sources. Considering only sources that are detected in the X-ray band, NLSy1 galaxies are less optically variable than BLSy1 galaxies. The amplitude of variability in the sample of both NLSy1 and BLSy1 galaxies is found to be anti-correlated with Fe II strength but correlated with the width of the Hβ line. The well-known anti-correlation of variability–luminosity and the variability–Eddington ratio is present in our data. Among the radio-loud sample, variability amplitude is found to be correlated with radio-loudness and radio-power, suggesting that jets also play an important role in the OV in radio-loud objects, in addition to the Eddington ratio, which is the main driving factor of OV in radio-quiet sources.

Key words: galaxies: active – galaxies: Seyfert – techniques: photometric

1. Introduction

Active galactic nuclei (AGNs) are among the luminous extragalactic sources in the sky persistently emitting radiation with bolometric luminosities as large as 10^{48} erg s^{-1} (Woo & Urry 2002). They are believed to be powered by accretion of matter onto supermassive black holes (SMBH) at the center of galaxies (Lynden-Bell 1969; Rees 1984). A small fraction ($\sim$15%) of AGNs are radio-loud and emit in the radio band, thereby possessing powerful relativistic jets (Kellermann et al. 1989). One of the important observed characteristics of all categories of AGNs is that they show variations in their emitted flux. This was known since their discovery as a class of object (Greenstein 1963; Schmidt 1963). The flux variations in AGNs are random and occur on different timescales of minutes, hours, and days, and have been observed over all accessible wavelengths (Wagner & Witzel 1995; Ulrich et al. 1997).

In recent years, AGNs have been extensively studied for their optical variability (OV). Several theoretical models have been proposed to explain the observed flux variations such as accretion disk instabilities (Kawaguchi et al. 1998), multiple supernovae (Aretxaga et al. 1997), micro-lensing (Hawkins 2000), Poisson process (Cid Fernandes et al. 2000), and damped random walk (DRW; Kelly et al. 2009). However, we still do not have an understanding of the underlying physical processes that cause flux variability. Extensive optical photometric monitoring of large samples of AGNs has revealed important connections between the observed variability and the various important physical properties of the sources. Some of the observed correlations are the dependency of the amplitude of variability with wavelength (di Clemente et al. 1996), luminosity (Hook et al. 1994; Kelly et al. 2009; Meusinger et al. 2011), redshift (Vanden Berk et al. 2004; Meusinger et al. 2011), black hole mass, and Eddington ratio (Wold et al. 2007; Bauer et al. 2009; Kelly et al. 2009; MacLeod et al. 2010). Variability is thus an important tool for investigating the complex nature of the central engine and accretion processes in AGNs.

Past variability studies mainly focused on broad-line AGNs; however, only limited reports are available in the literature on the OV characteristics of narrow-line Seyfert 1 (NLSy1) galaxies. NLSy1 galaxies are a peculiar type of Seyfert 1 galaxy with an FWHM of the broad permitted line FWHM(Hβ) < 2000 km s^{-1} and a flux ratio of [O III] to H$\beta < 3$ (Osterbrock & Pogge 1985; Goodrich 1989). They usually show stronger Fe II emission compared to their broad-line counterparts (Véron-Cetty et al. 2001). NLSy1 galaxies also show stronger soft X-ray variability and steeper X-ray spectra than BLSy1 galaxies (Leighly 1999b; Grupe 2004). They harbor low-mass black holes (10^6–$10^8\,M_\odot$) and have high Eddington ratios compared to the BLSy1 galaxies that are believed to be hosted by heavier ($\gtrsim 10^8\,M_\odot$) black holes (Zhou et al. 2006; Xu et al. 2012). However, recent studies indicate that NLSy1 galaxies do have black hole masses similar to those of blazars (Calderone et al. 2013; Baldi et al. 2016). Several authors have studied the reasons for mass deficit in NLSy1 galaxies and suggest geometrical factors to be the reason for observing narrow emission lines and consequently low black hole mass determination from virial estimates (Decarli et al. 2008; Calderone et al. 2013; Liu et al. 2016). Though there are some differences in the observed properties of BLSy1 and NLSy1 galaxies, we do not yet have a clear picture on the similarities and/or differences in the OV properties between these two classes of objects. A comparative analysis of the OV properties of BLSy1 and NLSy1 galaxies could provide clues to the cause of the peculiar observational characteristics of NLSy1 galaxies.

Though NLSy1 galaxies have not been studied extensively for optical variability, a few studies do exist in the literature. Such studies, though limited in number, have focused on flux variations within a night (Young et al. 1999; Miller et al. 2000) as well as on timescales of days (Young et al. 1999; Miller et al. 2000). Doroshenko et al. (2006) performed long-term optical photometric monitoring of a NLSy1 galaxy Ark 564

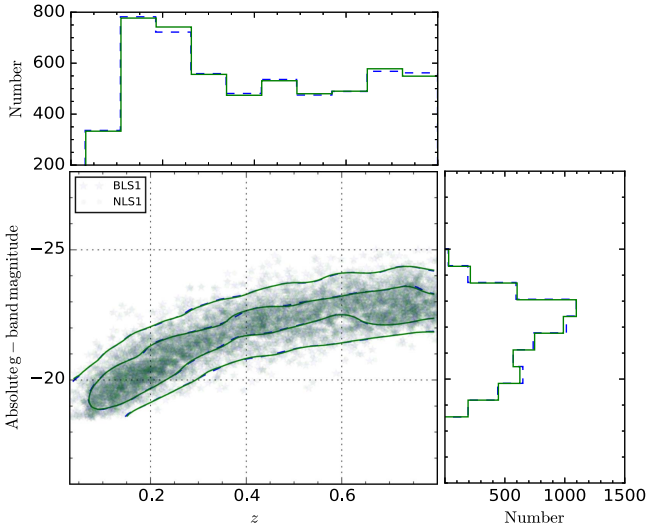

Figure 1. Absolute g-band magnitude (M_g) against redshift (z) for BLSy1 galaxies (dashed contours) and NLSy1 galaxies (solid contours). The contours are the 68 and 95 percentile density contours. The corresponding distribution of z (top) and M_g (right) is also shown. Both NLSy1 galaxies (solid line) and BLSy1 galaxies (dashed line) have similar distributions.

and found a low variability amplitude of 0.1–0.2 mag. Similar results have also been found by Klimek et al. (2004), who studied six NLSy1 galaxies and concluded that NLSy1 galaxies as a class show less variability than BLSy1 galaxies, and the extreme variability seen in the soft X-ray is not present in the optical. Both these studies lack a proper sample of NLSy1 galaxies. Benefiting from the Sloan Digital Sky Survey (SDSS) multi-wavelength, multi-epoch-repeated photometric data and the extended catalog of NLSy1 galaxies compiled by Zhou et al. (2006), a comparative study of NLSy1 and BLSy1 galaxies with a moderate sample of 55 NLSy1 galaxies and a control sample of 108 BLSy1 galaxies was first made by Ai et al. (2010) and subsequently by Ai et al. (2013). They found: (1) NLSy1 galaxies have systematically smaller variability than BLSy1 galaxies; (2) the amplitude of variability increases with the width of Hβ and strength of [O III] lines but decreases with the strength of Fe II emission; (3) variability is anti-correlated with Eddington ratio but insignificant with luminosity; and (4) a positive correlation with black hole mass is found, but vanishes after controlling for Eddington ratio in the analysis, which the authors noted could be due to the limited ranges of luminosity and black hole mass of their sample. However, these findings are based on the poorly sampled SDSS photometric light curves having only about 27 observations over a duration of 5 years.

Earlier studies on the OV of a large sample of NLSy1 galaxies were limited because (i) a small number of NLSy1 galaxies known at that time and (ii) the lack of long-term photometric data. Recently, Rakshit et al. (2017) compiled a new catalog of NLSy1 galaxies consisting of 11,101 sources, which is a factor of five increase in the number of NLSy1 galaxies from the previous catalog. During the course of NLSy1 galaxies selection, Rakshit et al. (2017) also arrived at a large sample of BLSy1 galaxies. Long-term V-band observations of many of these objects are available from the Catalina Real Time Transient Survey (CRTS; Drake et al. 2009). Motivated by the availability of a large sample of BLSy1 and NLSy1 galaxies and the CRTS data, we carried out a comparative study of OV of both BLSy1 and NLSy1 galaxies to understand the correlation of variability amplitude with different physical characteristics of these two populations of sources. In this paper, we present the results of this study. This paper is organized as follows. In Section 2, we present the sample of NLSy1 and BLSy1 galaxies and the photometric data used for this study, followed by an analysis in Section 3. The results are given in Section 4, followed by a summary and conclusions in Section 5. A cosmology with $H_0 = 70\ \mathrm{km\ s^{-1}\ Mpc^{-1}}$, $\Omega_\mathrm{m} = 0.3$, and $\Omega_\lambda = 0.7$ is assumed throughout.

2. Sample and Data

2.1. NLSy1 and BLSy1 Galaxies Sample

Our sample of NLSy1 galaxies is taken from Rakshit et al. (2017). This was extracted from a systematic re-analysis of the spectra of objects in SDSS DR12 (Alam et al. 2015) that are classified as "QSO" by the automatic SDSS spectroscopic pipeline (Richards et al. 2002). The custom emission-line-fitting process by Rakshit et al. (2017) to identify new NLSy1 galaxies from the SDSS DR12 database also allowed them to compile a sample of BLSy1 galaxies that have FWHM (Hβ) $> 2200\ \mathrm{km\ s^{-1}}$. Since the number of BLSy1 galaxies is very large, for this work, we created a subsample of BLSy1 galaxies with median SNRs $> 10\ \mathrm{pixel^{-1}}$ in the SDSS spectra, resulting in 14,894 BLSy1 galaxies. Thus, the sample of sources selected for this study consists of 11,101 NLSy1 galaxies and 14,894 BLSy1 galaxies.

2.2. Photometric Data

For OV studies of the sample selected above, we used the data from CRTS[1] (Drake et al. 2009). It provides light curves with much higher temporal sampling, thereby enabling us to study the variability characteristic of our sample (Graham et al. 2015). CRTS streams data from three telescopes; the 0.7 m Catalina Schmidt Telescope with a field of view of 8 $\mathrm{deg^2}$, the 1.5 m Mount Lemmon Survey reflector telescope having a 1 $\mathrm{deg^2}$ field of view located north of Tucson, Arizona, and the 0.5 m Uppsala Schmidt telescope at Siding Spring, Australia having a 4.2 $\mathrm{deg^2}$ field of view. CRTS covers about 2500 $\mathrm{deg^2}$ sky per night taking 4 exposures per visit that are separated by 10 minutes. Observations are made over 21 nights per lunation, reaching a V-band magnitude of around 19–20 mag. All data are processed in real time using an automated software and calibrated to the Johnson V-band. CRTS data contain light curves of about 500 million sources. Detailed information regarding the CRTS survey and the optical light curves can be found in Drake et al. (2009, 2013) and Graham et al. (2015).

We cross-correlated our sample of sources with CRTS within a search radius of 3″. This cross-correlation yielded optical light curves for a reduced sample of 9069 NLSy1 galaxies and 13,928 BLSy1 galaxies. A common practice in dealing with light curves obtained in large surveys is to identify and consequently remove any spurious outliers that might have been caused by photometric or technical errors. To remove such outliers we applied an iterative 3σ clipping algorithm around the local group of data points to all the light curves. For any given light curve we removed points with more than 3σ deviation from the mean and repeat this process until no points with 3σ deviation are present in the light curve or the number of points in the light curve between two consecutive iterations

[1] http://nesssi.cacr.caltech.edu/DataRelease

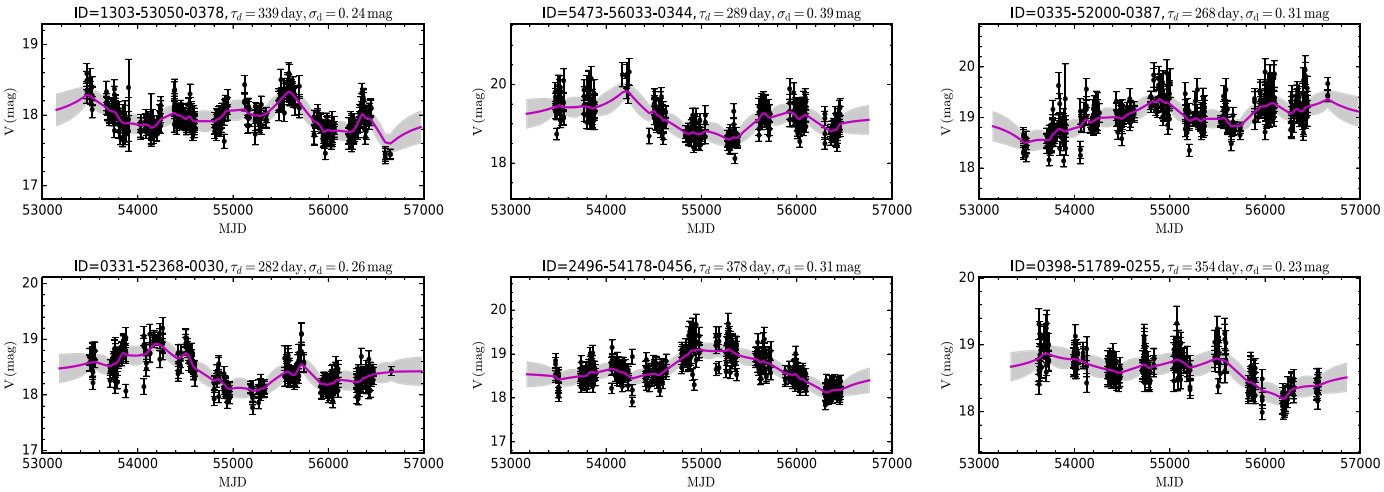

Figure 2. Examples of light-curve fitting using JAVELIN. The black points with error bars are the CRTS data and the solid line shows the best fit of the light curve, while the shaded area is the 1σ error region. The SDSS ID (plate-MJD-fiber) and the JAVELIN best-fitted parameters (observed frame) are noted in each panel.

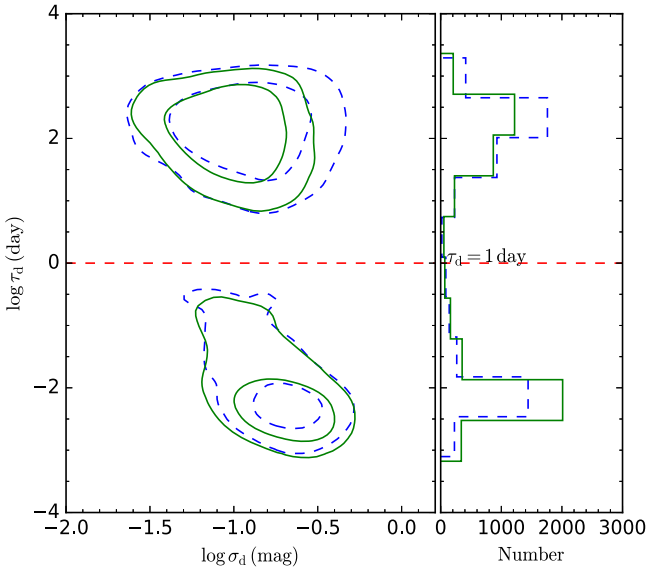

Figure 3. Distribution of JAVELIN best-fitted parameters, the rest-frame damping timescale (τ_d), and the observed frame amplitude of variation σ_d, as obtained from the fitting NLSy1 galaxies (solid contours) and BLSy1 galaxies (dashed contours) in the τ_d–σ_d plane. The shown contours are the 68 and 95 percentile density contours. The horizontal dashed line indicates $\tau_d = 1$. The distribution of τ_d (1D cut along the y-axis) is shown in the left panel for NLSy1 (solid line) and BLSy1 (dashed line) galaxies.

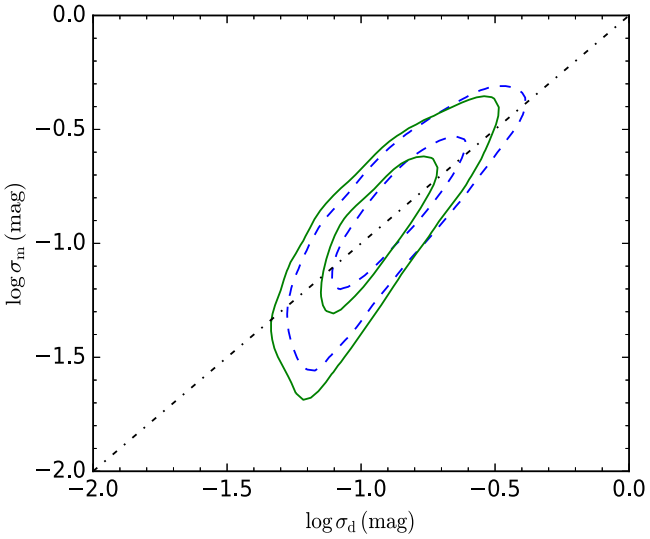

Figure 4. Comparison between two variability amplitude indicators, σ_m and σ_d, in the observed frame for NLSy1 galaxies (solid contours) and BLSy1 galaxies (dashed contours). The shown contours are the 68 and 95 percentile density contours. The dashed–dotted line represents one-to-one correspondence between σ_m and σ_d.

remain the same. Since our aim is to study OV, we further considered only those light curves that have a minimum of 50 epochs of data. This brings down the sample size to 9063 NLSy1 and 13,831 BLSy1 galaxies.

The motivation of this work is to carry out a systematic comparative study of the OV properties between NLSy1 and BLSy1 galaxies. It is therefore imperative that the sample selected must match as close as possible to each other in the luminosity–redshift plane. For that, we divided both the samples in small redshift and luminosity bins, and randomly selected an equal number of NLSy1 and BLSy1 galaxies from each bin. This resulted in a final working sample of 5510 NLSy1 and 5510 BLSy1 galaxies. The distribution of the sample of NLSy1 and BLSy1 galaxies ($z < 0.8$) in the luminosity–redshift plane is shown in Figure 1. From the figure, it is evident that both samples of galaxies resemble each other. The two-dimensional Kolmogorov-Smirnov (K–S) test (Press et al. 1992) yields a statistics of 0.007 and a p-value of 0.98, confirming that both samples have the same $M_g - z$ distribution.

3. Analysis of Variability

The CRTS V-band[2] light curves of the sources studied for variability contain a minimum of 50 epochs of data and the total duration of the light curves spans 5–9 years. Various studies show that the OV of quasars can be well described by a

[2] The V-band has an effective wavelength ($\lambda_{\rm eff}$) of 5510 Å, with a bandwidth of 880 Å, this covering a wavelength range of 4630 Å to 6390 Å. It can thus be contaminated by strong broad emission lines such as redshifted Mg II ($\lambda_{\rm eff} = 2800$ Å) and Hβ ($\lambda_{\rm eff} = 4861$ Å), which also vary with time and follow the nuclear continuum variations. Since our sample spans $z = 0$ to 0.8, Hβ will contribute to the V-band flux for the objects with $z < 0.31$, while Mg II will contribute for objects with $z > 0.65$. Therefore, it is very difficult to disentangle the relative contribution of broad emission lines and the continuum to the broad V-band photometry.

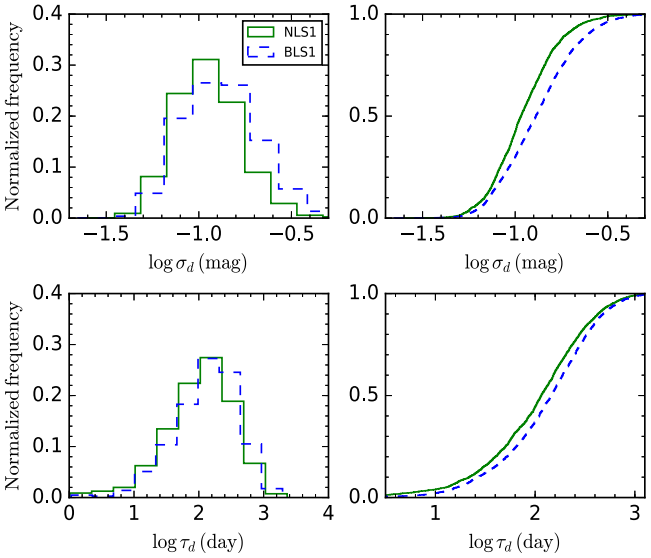

Figure 5. Upper panel: the distribution of variability amplitude (σ_d; left panel) and its cumulative distribution (right panel). Lower panel: the same for the characteristic timescale of variability. The solid line is for NLSy1 galaxies and the dashed line is for BLSy1 galaxies.

damped random walk (DRW; Kelly et al. 2009), which is a stochastic process with an exponential covariance function

$$S(\Delta t) = \sigma_d^2 \exp\left(-\frac{|\Delta t|}{\tau_d}\right), \quad (1)$$

where σ_d is the amplitude and τ_d is a characteristic timescale of variability (Kozłowski et al. 2010; MacLeod et al. 2010; Zu et al. 2011, 2013, 2016). DRW is shown to provide a realistic explanation of quasar OV and both the model parameters, σ_d and τ_d, are correlated with the physical parameters of AGNs, such as luminosity, black hole mass, and Eddington ratio (Kelly et al. 2009; Kozłowski et al. 2010; MacLeod et al. 2010; Andrae et al. 2013; Kozłowski 2016c). The DRW model is a powerful tool for quantifying variability characteristics on timescales of several days to years, although recently some limitations of the DRW model have been noticed, especially when dealing with light curves that have observation durations about ten times shorter than the true DRW timescale (Kozłowski 2016a, 2016b).

To quantify the variability characteristics of all the sources in our sample, we fit each of their *V*-band CRTS light curves using the DRW model implemented in JAVELIN[3], which is a python code developed by Zu et al. (2011). Logarithmic priors for both τ_d and σ_d have been used for fitting the light curves. JAVELIN has been used widely in the literature to model the continuum and line emission light curves of AGN reverberation mapping data (Grier et al. 2012; Pancoast et al. 2014). Few examples of fitting done on the light curves are shown in Figure 2. The estimated values of the parameters after fitting all light curves are plotted in Figure 3, where τ_d is the rest-frame timescale i.e., the timescale of variability corrected for the redshift. A bimodal distribution along the time axis is clearly visible and delineated by a gap at about 1 day. Since the time sampling of CRTS is greater than 1 day, any variability on timescales shorter than 1 day is unreliable and cannot be used for variability analysis. Also, these sources have poor-quality light curves with no noticeable variability trend, as confirmed by visual examinations. Therefore, only objects with τ_d greater than 1 day were considered for further variability analysis. This leads us to a sample of 2161 (39.2%) NLSy1 and 2919 (52.9%) BLSy1 galaxies for further variability analysis. This also suggests that only 39% of NLSy1 galaxies from our original sample are variable, while 61% NLSy1 galaxies are non-variable on timescales larger than 1 day. However, in the case of BLSy1 galaxies, about 53% of our original sample is variable, which implies that overall, BLSy1 galaxies are more variable than NLSy1 galaxies on timescales longer than 1 day.

Following Ai et al. (2010), we also calculated the intrinsic amplitude of variability (σ_m). This was estimated from the measured variance of the observed light curves after subtracting the measurement errors. The σ_m is estimated using the following formalism (see Sesar et al. 2007):

$$\Sigma = \sqrt{\frac{1}{n-1}\sum_{i=1}^{N}(m_i - \langle m \rangle)^2}, \quad (2)$$

where $\langle m \rangle$ is the weighted average and the amplitude of variability σ_m is

$$\sigma_m = \begin{cases} \sqrt{\Sigma^2 - \epsilon^2}, & \text{if } \Sigma > \epsilon, \\ 0, & \text{otherwise.} \end{cases}$$

Here, ϵ represents the contribution of measurement errors to the variance and it is estimated directly from the errors of individual observed magnitudes ϵ_i,

$$\epsilon^2 = \frac{1}{N}\sum_{i=i}^{N}\epsilon_i^2. \quad (3)$$

In Figure 4, we show the two indicators of variability amplitude for our sample of sources, σ_d obtained from fitting the light curves using JAVELIN, and σ_m estimated directly from the observed light curves. The dashed–dotted line indicates one-to-one correspondence between the two values. In this work, we used σ_d as the indicator of the amplitude of variation unless specified otherwise.

4. Results

4.1. NLSy1 Versus BLSy1 Galaxies

We compare the variability amplitudes and timescales for the 2161 NLSy1 and 2919 BLSy1 galaxies in Figure 5. The normalized histogram (left panel) and cumulative distribution (right panel) of variability amplitude are shown in the upper panels, while the same parameters for timescales are shown in the lower panels. The σ_d distribution has a median of $0.107^{+0.057}_{-0.032}$ mag and $0.129^{+0.082}_{-0.049}$ mag for NLSy1 and BLSy1 galaxies, respectively. When σ_m distribution is considered, we find the median values are $0.112^{+0.089}_{-0.056}$ and $0.136^{+0.114}_{-0.069}$ for NLSy1 and BLSy1 galaxies, respectively. Within errors, the median amplitudes of variability found in BLSy1 and NLSy1 are similar; however, a two-sample K–S test applied to the distribution of σ_d for NLSy1 and BLSy1 galaxies yields a *D*-statistic value of 0.17 and *p*-value of 6×10^{-31}, confirming that the two distributions are significantly different. NLSy1 galaxies as a class are thus less variable than BLSy1 galaxies. Therefore, the strong variability shown by NLSy1 galaxies in X-rays relative to BLSy1 galaxies is not seen in the optical

[3] http://bitbucket.org/nye17/javelin

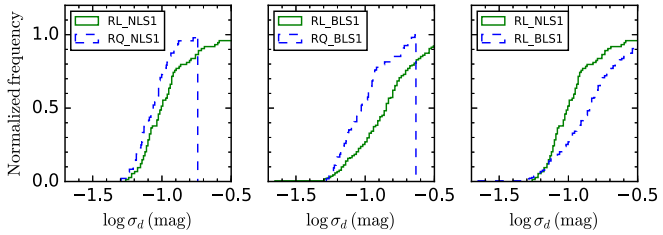

Figure 6. Cumulative distribution of radio-loud NLSy1 vs. radio-quiet NLSy1 galaxies (left), radio-loud BLSy1 vs. radio-quiet BLSy1 galaxies (middle), and radio-loud NLSy1 vs. radio-loud BLSy1 galaxies (right). The solid and dashed lines are for NLSy1 and BLSy1 galaxies, respectively.

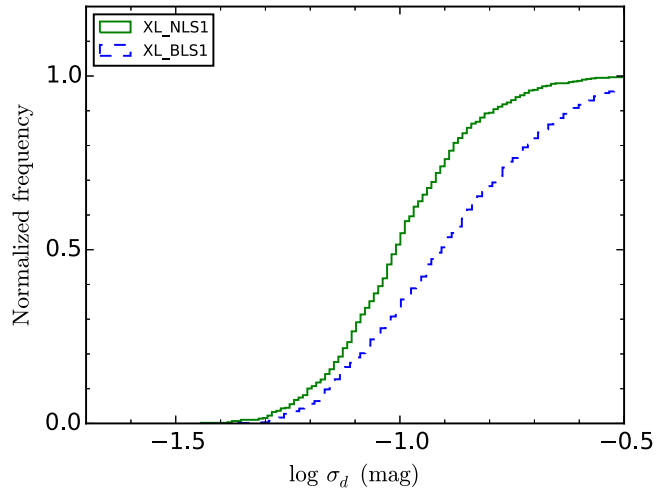

Figure 7. Cumulative distribution of X-ray-detected BLSy1 (dashed line) and NLSy1 (solid line) galaxies.

band. The distribution of timescales for NLSy1 galaxies has a peak slightly smaller than that of BLSy1 galaxies, having a median value of 116^{+207}_{-83} days. This is smaller than the median value of 146^{+235}_{-104} days found in BLSy1 galaxies, though the scatter in the distribution is very large. A two-sample K–S test of τ_d distribution for NLSy1 and BLSy1 galaxies yields a D-statistic value of 0.09 and p-value of 2×10^{-8}. Because the D-statistics is small it is difficult to draw any conclusion on the distribution of τ_d between NLSy1 and BLSy1 galaxies. According to Kozłowski (2016b), for reliable estimation of τ_d, one needs to have data with a minimum duration of about 10 times longer than the true DRW timescale. As our data span 5 to 9 years, about 18% of NLSy1 galaxies and 24% of BLSy1 galaxies have the duration of light curve $<10 \times \tau_d$. Thus, for those light curves τ_d may not represent the true timescale. However, σ_d is independent of the duration of light curves and only affected by the photometric noise. As our main motivation is to have a comparative analysis of the amplitude of variability (σ_d) of NLSy1 and BLSy1 galaxies, we restricted ourselves to further analysis of σ_d only.

This study, using a matched sample of NLSy1 and BLSy1 galaxies, has clearly demonstrated the difference in their OV properties, with NLSy1 galaxies showing lower variability amplitude than BLSy1 galaxies. This finding is consistent with the results of Klimek et al. (2004), who studied OV using a small sample and the ensemble variability study of Ai et al. (2010, 2013), who analyzed a sample of 55 NLSy1 galaxies and a control sample of 108 BLSy1 galaxies. The weaker variability of NLSy1 galaxies compared to BLSy1 galaxies can be understood in terms of them having smaller width and stronger Fe II emission compared to BLSy1 galaxies. As accretion disks are normally thought to be responsible for optical/UV radiation from AGNs, the difference in the OV properties leads us to speculate on the differences in the physical processes operating in the accretion disks of NLSy1 and BLSy1 galaxies. One possibility could be the slim disk scenario in NLSy1 galaxies compared to the standard Shakara-Sunyaev, geometrically thin optically thick accretion disk in BLSy1 galaxies (Ai et al. 2013).

4.2. Radio Subsample

The observed optical emission from radio-loud and radio-quiet objects can be due to a combination of different physical processes. One of the ways to ascertain this is to see if there is any difference in the OV properties of both NLSy1 and BLSy1 galaxies when they are subdivided based on their radio properties. We therefore cross-correlated our sample of NLSy1 and BLSy1 galaxies with the Faint Images of the Radio Sky at Twenty centimeters (FIRST)[4] catalog (Becker et al. 1995) within a search radius of 2″. We found that 122 out of 2161 NLSy1 galaxies and 276 out of 2919 BLSy1 galaxies are detected in FIRST. Depending on their radio-loudness (defined as the logarithmic flux ratio of 1.4 GHz to g-band flux, i.e., $R = f_{1.4\,\mathrm{GHz}}/f_g$), we further divided the radio-detected NLSy1 and BLSy1 galaxies into radio-quiet (RQ; $\log R < 1$) and radio-loud (RL; $\log R > 1$) sub-categories. This resulted in 48 (54) radio-quiet and 74 (222) radio-loud NLSy1 (BLSy1) galaxies.

The cumulative distributions of their σ_d values are plotted in Figure 6. In both NLSy1 and BLSy1 galaxies (left and middle), radio-loud objects show more variability than their radio-quiet counterparts. Comparing the radio-loud sample of both NLSy1 and BLSy1 galaxies (right panel), we found that RL-BLSy1 galaxies are more variable than RL-NLSy1 galaxies. The median values of σ_d distributions are $0.100^{+0.067}_{-0.025}$ ($0.144^{+0.107}_{-0.065}$) mag and $0.087^{+0.026}_{-0.021}$ ($0.094^{+0.060}_{-0.029}$) mag for RL-NLSy1 (RL-BLSy1) and RQ-NLSy1 (RQ-BLSy1) galaxies, respectively. When the median variability amplitudes are compared, we find that within error bars, both radio-loud and radio-quiet sources have similar variability amplitudes. However, a K–S test indicates that their intrinsic distributions are different. A two-sample K–S test applied on the σ_d distributions of RL-NLSy1 and RQ-NLSy1, RL-BLSy1 and RQ-BLSy1, as well as RL-NLSy1 and RL-BLSy1 galaxies, yield p-values of 4×10^{-2} (D-statistics = 0.25, left panel), 1×10^{-6} (D-statistics = 0.39, middle panel), and 6×10^{-7} (D-statistics = 0.36, right panel), respectively, confirming that the distributions are different. Therefore, the OV of radio-loud sources must be due to some other mechanisms, in addition to variations caused due to accretion disk instabilities that operate in radio-quiet sources.

4.3. X-Ray Subsample

NLSy1 galaxies are known to show stronger soft X-ray variability than their broad-line counterparts (Leighly 1999a; Grupe 2004). To ascertain if this nature of NLSy1 galaxies also holds true in their OV properties, we created a subsample of X-ray-detected (XL) NLSy1 and BLSy1 galaxies from the work of Rakshit et al. (2017). A total of 577 NLSy1 galaxies and 653 BLSy1 galaxies, out of 2161 NLSy1 galaxies and 2919

[4] http://sundog.stsci.edu

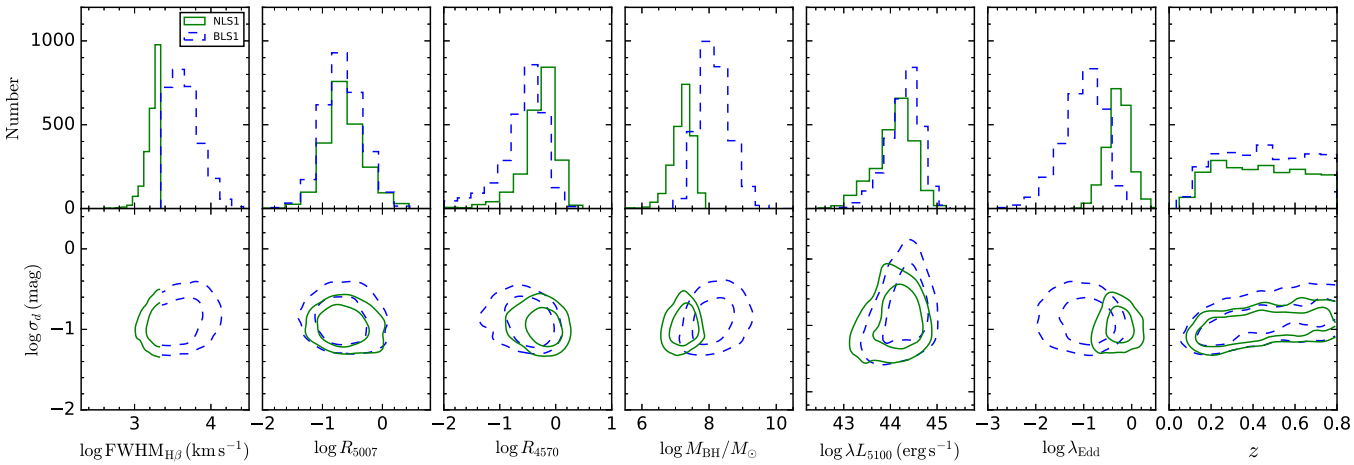

Figure 8. From right to left, the correlations of σ_d with FWHM$_{H\beta}$, R_{5007}, R_{4570}, M_{BH}, λL_{5100}, λ_{Edd}, and z are plotted in the lower panels. The upper panels show the distribution of the parameters of all the objects in the sample, i.e., the cut of the lower panels along the x-axis. The dashed contours represent BLSy1 galaxies, while the solid contours correspond to NLSy1 galaxies. The shown contours are the 68 and 95 percentile density contours.

Table 1
Correlation of Amplitude of Variability (σ_d) with Different AGN Parameters

Test (1)	Sample (2)	Size (3)	FWHM(Hβ) (4)	R_{5007} (5)	R_{4570} (6)	log $M_{BH}/M_\odot$ (7)	log λL_{5100} (8)	log λ_{Edd} (9)	z (10)
σ_d-	NLSy1	2161	+0.07(4e−04)	−0.08(1e−04)	−0.17(7e−15)	+0.13(1e−09)	+0.08(7e−05)	0.00(9e−01)	+0.35(3e−65)
	BLSy1	2919	+0.18(9e−25)	−0.08(2e−06)	−0.23(2e−37)	+0.27(3e−50)	+0.23(4e−38)	−0.07(2e−05)	+0.44(9e−137)
	All	5080	+0.22(2e−60)	−0.09(3e−11)	−0.25(3e−73)	+0.27(3e−86)	+0.21(3e−55)	−0.16(1e−30)	+0.40(1e−200)

Note. The columns are as follows: (1) variability parameters; (2) sample; (3) size of the sample. Columns (4)–(10) note the Spearman correlation coefficient (the p-value of no correlation) for the width of the Hβ line, R_{5007}, R_{4570}, log $M_{BH}/M_\odot$, log λL_{5100}, log λ_{Edd}, and redshift (z).

BLSy1 galaxies, are detected in the second *ROSAT* all-sky (2RXS) source catalog (Boller et al. 2016). The cumulative distribution of their σ_d values is shown in Figure 7. The σ_d distribution has a median of $0.099^{+0.043}_{-0.027}$ mag and $0.124^{+0.084}_{-0.047}$ mag for XL-NLSy1 and XL-BLSy1 galaxies, respectively. A two-sample K–S test confirms distributions to be significantly different (D-statistics = 0.25 and p-value = 2×10^{-18}). Hence, the XL-BLSy1 galaxies are more variable than the XL-NLSy1 galaxies. As the high flux variation shown by NLSy1 galaxies relative to BLSy1 galaxies in the X-ray band is not seen in the OV light curves, it is clear that the physical processes causing the X-ray flux variation and OV are different.

4.4. Correlation of Variability and Emission-line Parameters

The work of Rakshit et al. (2017) has yielded various emission-line parameters of the sources in our sample. To understand how variability is related to the key physical properties of AGNs, we tested several correlations between variability and various physical characteristics of the sources such as FWHM(Hβ), the strength of the [O III] line (defined as $R_{5007} = F_{[O\,III]}(5007\,\text{Å})/\text{H}\beta_{tot}$), the Fe II strength relative to Hβ (defined as $R_{4570} = \text{Fe II}(\lambda 4434\text{–}4684)/\text{H}\beta_b$), and the monochromatic luminosity at 5100 Å (λL_{5100}). All these parameters were taken from the work of Rakshit et al. (2017). In Figure 8, the distributions of individual parameters are shown in the top panel, while in the bottom panel their correlations with σ_d are shown. Table 1 summarizes the Spearman's rank correlation coefficient and the two-sided p-values for the null hypothesis of no correlation.

The amplitude of variability is positively correlated with the width of Hβ line but negatively correlated with R_{4570}. Spearman's rank correlation test confirms both the correlations to be significant. The above correlations are found to remain when all the sources are considered together or separately for the sample of BLSy1 and NLSy1 galaxies. The strong anti-correlation of variability amplitude with R_{4570} found here implies a lower variability in NLSy1 than BLSy1 galaxies, since the former has stronger Fe II emission than the latter. However, no correlation between σ_d and R_{5007} has been found. These results are consistent with the findings of Ai et al. (2010), although their sample is very small compared to this work. It is likely that the low amplitude of variability in NLSy1 galaxies compared to BLSy1 galaxies is an outcome of the correlation seen between σ_d and the width of the Hβ line and R_{4570}. A positive correlation is also found between σ_d and λL_{5100}.

4.5. Dependence of Variability with Redshift

Though the redshift range of this study is limited to $z < 0.8$ (demanded by the presence of both Hα and Hβ in the SDSS spectra; Rakshit et al. 2017), a strong positive correlation is found between σ_d and z, with a Spearman's rank correlation coefficient of 0.40 and p-value of 1×10^{-200}, with the high-z sources showing larger amplitudes of variability than their low -z counterparts. This is the strongest correlation among all the other correlations investigated here. Such redshift evolution of variability was also noticed in quasars by Vanden Berk et al. (2004) up to $z \sim 5$, although Kozłowski et al. (2010) and MacLeod et al. (2010) found a negligible trend with redshift,

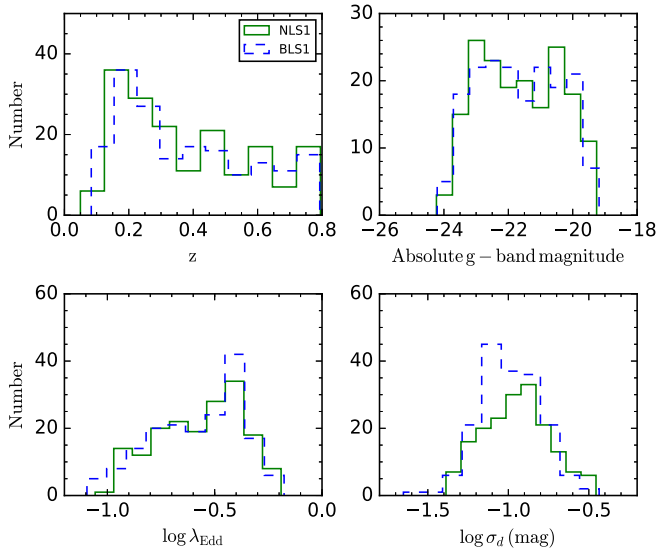

Figure 9. Distribution of z (upper left), M_g (upper right), λ_{Edd} (lower left), and σ_d (lower right) for a subsample of NLSy1 (solid) and BLSy1 (dashed) galaxies.

suggesting that the variability is intrinsic to the quasar and does not evolve over cosmic time for fixed physical parameters of the quasars (black hole mass, absolute magnitude etc.). Since AGNs are more variable at shorter wavelengths, the positive correlation observed between σ_d and z in this work is most likely a manifestation of the anti-correlation known to exist between variability and wavelength (Cid Fernandes et al. 1996) because higher redshifts probe shorter rest-frame wavelengths.

4.6. Dependence of Variability with M_{BH}

In the process of selecting new NLSy1 galaxies, Rakshit et al. (2017) carried out spectral fitting of SDSS spectra for all the candidates selected in their study. The results of that fitting were used to derive the black hole masses of each of the sources, assuming a virial relationship using the following equation:

$$M_{BH} = f R_{BLR} \Delta v^2 / G, \quad (4)$$

where, Δv is the FWHM of the broad component of the Hβ emission line and f is a scale factor that depends strongly on the geometry and kinematics of the BLR (Rakshit et al. 2015). Considering the spherical distribution of clouds, we used $f = 3/4$. In Figure 8 the correlation between variability amplitude and BH mass is shown. It is clear from the figure that σ_d is positively correlated with M_{BH}. The positive correlation found here between σ_d–M_{BH} is consistent with Wold et al. (2007), Wilhite et al. (2008), and Ai et al. (2010). However, Ai et al. (2010) found the correlation to vanish when the dependency of λ_{Edd} is considered in the relation. Li & Cao (2008) suggested that such a positive correlation between variability amplitude and black hole mass can be explained in terms of an accretion disk model having the mean accretion rate of $\dot{m}_o = 0.1$ and a variation of 0.1–0.5$\dot{m}_o$.

4.7. Dependence of Variability with Eddington Ratio

The Eddington ratio, defined as the ratio of the bolometric luminosity to Eddington luminosity, is a very important physical parameter that characterizes the accretion rate of an AGN. For the sources in our sample, Eddington ratio (λ_{Edd}) is estimated as

$$\lambda_{Edd} = L_{bol} / L_{Edd}, \quad (5)$$

where $L_{bol} = 9 \times \lambda L_\lambda(5100\,\text{Å})\,\text{erg s}^{-1}$ and $L_{Edd} = 1.3 \times 10^{38} M_{BH}/M_\odot\,\text{erg s}^{-1}$ (Kaspi et al. 2000). The correlation between σ_d and λ_{Edd} is shown in Figure 8, wherein an anti-correlation is observed. This correlation will have effects due to uncertainties in calculation of M_{BH} and consequently L_{Edd}. Such a correlation is also observed by Kelly et al. (2009), MacLeod et al. (2010), Ai et al. (2010), and many others. It has been shown by Ai et al. (2010) that the correlation between σ_d and λ_{Edd} remains significant even after taking the dependency of M_{BH}, leading them to conclude the existence of a robust negative correlation between σ_d and λ_{Edd}.

To study the effect of λ_{Edd} on σ_d, we created a subsample of 176 NLSy1 and BLSy1 galaxies, respectively, matching as close as possible their z, M_g, and λ_{Edd}. The distributions of z (upper left), M_g (upper right), and λ_{Edd} (lower left) for this subsample of NLSy1 (solid) and BLSy1 (dashed) galaxies are shown in Figure 9. The distributions look similar. A K–S test gave D-statistics (p-values) of 0.04 (0.99), 0.05(0.93), and 0.05 (0.93) for the distributions of z, M_g, and λ_{Edd}, that indicates no differences in the distributions of z, M_g, and λ_{Edd} between the subsamples of NLSy1 and BLSy1 galaxies. Also, the distribution of σ_d (lower right) for this subsample is shown in Figure 9. A two-sample K–S test applied to the distributions of σ_d for this subsample of NLSy1 and BLSy1 galaxies gives a D-statistics and p-value of 0.10 and 0.30, respectively, indicating that this subsample of NLSy1 and BLSy1 galaxies has similar σ_d distributions. Therefore, when matched in λ_{Edd}, both NLSy1 and BLSy1 galaxies are indistinguishable in their amplitude of OV. However, when considering the full sample of NLSy1 and BLSy1 galaxies, the larger amplitude of OV shown by BLSy1 galaxies relative to their NLSy1 counterparts is due to them having lower λ_{Edd} compared to NLSy1 galaxies, which is also manifested in the negative correlation between σ_d and λ_{Edd}.

The correlation between σ_d and λ_{Edd} found here can be understood from the simple standard accretion disk model (Shakura & Sunyaev 1973). If the emission originates from the inner accretion disk, the emission decreases as it propagates outward. As the Eddington ratio increases, the radius (r) of the emission region at a given wavelength moves outward, i.e., r increases with Eddington ratio since $r \sim T^{-1} \sim (\dot{m}/M_{BH})^{1/3} \lambda^{4/3}$, where T is the temperature of the disk, λ is the wavelength, and $\dot{m}$ is the mass accretion rate normalized by the Eddington rate. Since NLSy1 galaxies have higher a Eddington ratio compared to BLSy1 galaxies at a given wavelength, the size of the emission region is larger in NLSy1 galaxies than in BLSy1 galaxies, and thus variability amplitude is lower in the former than in the latter.

4.8. Variability versus Physical Parameters in Redshift Bins

To study the correlations mentioned in the earlier sections in detail, we further divided the sample into different redshift bins (z = 0.0–0.2, 0.2–0.4, 0.4–0.6, 0.6–0.8). All the correlations are shown in Figure 10 and the results of the correlation analysis are given in Table 2. It seems that at lower redshifts ($z < 0.4$), the correlation between σ_d and all the physical parameters investigated here is insignificant but for higher redshifts ($z > 0.4$), σ_d is strongly correlated with FWHM(Hβ), R_{4570}, λL_{5100}, and λ_{Edd}. σ_d increases with FWHM(Hβ) but

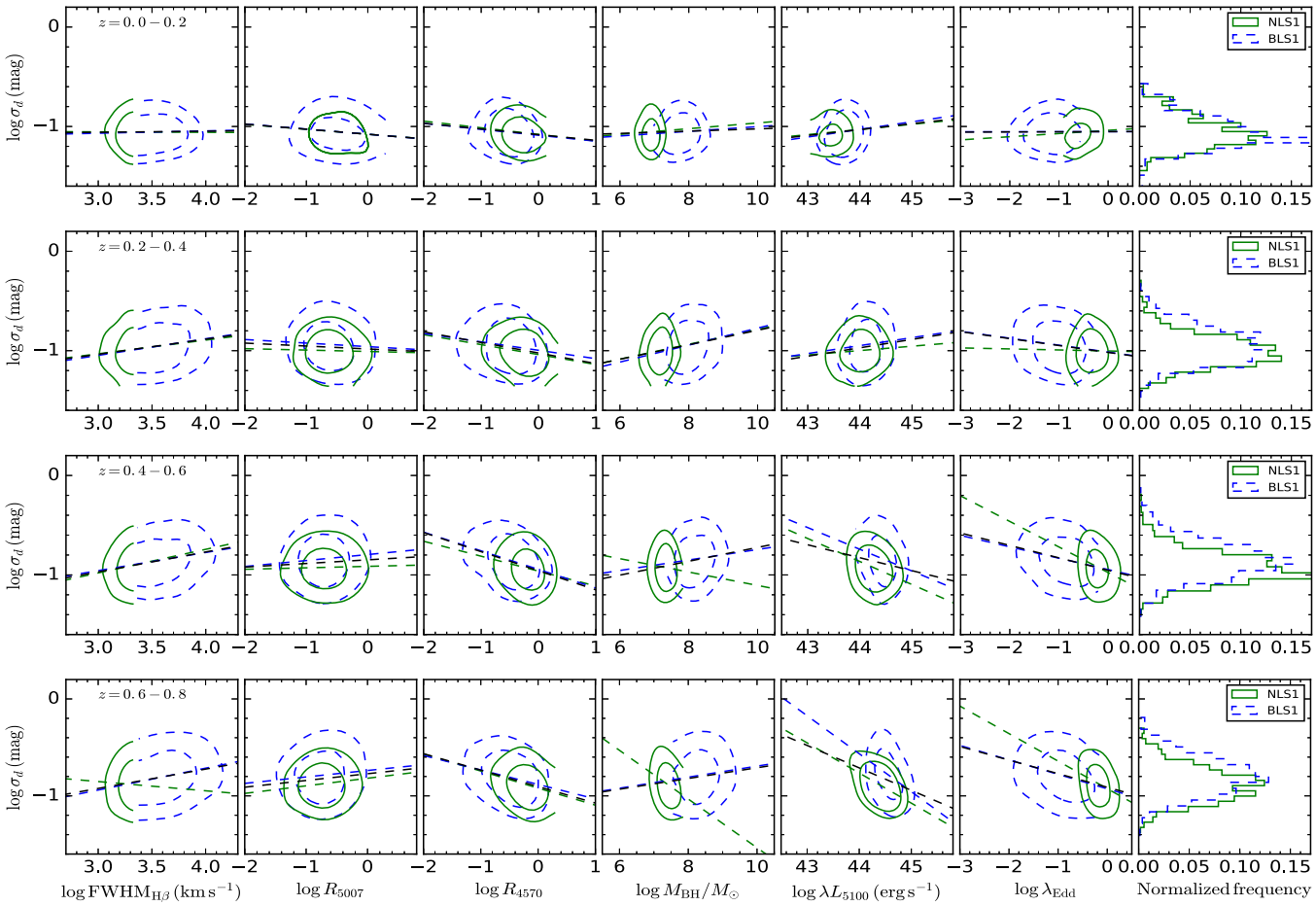

Figure 10. From right to left, the correlations of σ_d with $\mathrm{FWHM}_{\mathrm{H}\beta}$, R_{5007}, R_{4570}, M_{BH}, λL_{5100}, λ_{Edd}, and normalized distribution of σ_{d} are plotted for redshifts $z = 0.0$–0.2 (top), $z = 0.2$–0.4 (upper middle), $z = 0.4$–0.6 (lower middle), and $z = 0.6$–0.8 (bottom). The dashed contours represent BLSy1 galaxies, while the solid contours correspond to NLSy1 galaxies. The shown contours are 68 and 95 percentile density contours.

decreases with Fe II strength, luminosity, and Eddington ratio. Analyzing the correlation between σ_d and M_{BH} we found it to be weak when dividing all the objects in different redshift bins.

4.9. Correlation of Variability and Radio-loudness

A small subset of our sample of NLSy1 and BLSy1 galaxies has radio counterparts from the FIRST survey. In both populations, BLSy1 and NLSy1 galaxies, radio-loud sources are found to be more variable than radio-quiet sources (see Section 4.2). Though the Eddington ratio plays an important role, an additional mechanism might be at work in radio-loud objects. Since the origin of radio emission is relativistic jets, some contribution of it might influence the OV. In Figure 11, we plotted the variability amplitude against radio-loudness (left panel) and radio-power (right panel) for both NLSy1 and BLSy1 galaxies. Interestingly, a moderately strong correlation between variability amplitude and radio-loudness is found. This correlation is also present when the two samples are considered separately. The optical variability is also positively correlated with radio-power ($r = 0.36$ and p-value $= 8 \times 10^{-11}$), suggesting that objects with strong jets show a large amplitude of variation in the optical. The variation of σ_d with radio-loudness and radio-power can be explained by the following relations:

$$\log \sigma_d = (0.11 \pm 0.01)\log R + (-1.09 \pm 0.02), \quad (6)$$

$$= (0.09 \pm 0.01)\log P_{1.4} + (-4.51 \pm 0.56). \quad (7)$$

This finding leads us to hypothesize that the mechanisms for OV in radio-loud and radio-quiet objects can be quite different. It is likely that the optical emission in radio-quiet sources is due to the presence of both non-thermal emission from the jet in addition to the thermal emission from the accretion disk. Alternatively, in radio-quiet sources, the optical emission is due to accretion disk thermal emission.

5. Summary and Conclusion

We studied the OV of a large sample of NLSy1 and BLSy1 galaxies using archival V-band data from CRTS. The present study is a manifold increase compared to the earlier work in terms of (a) the number of objects used, (b) the epochs of data used for each of the objects, and (c) the duration of the observations. In this work we have used a sample of 5510 NLSy1 and 5510 BLSy1 galaxies that are well-matched in the $M_g - z$ plane. Each of these objects has a minimum of 50 epochs of data spanning 5 to 9 years. Therefore, the present sample, along with the rich data set, is ideal for a comparative study of the OV properties of NLSy1 and BLSy1 galaxies. The V-band light curves of our sample sources were modeled using DRW to understand their variability. From our sample, 2161 (39.2%) NLSy1 and 2919 (52.9%) BLSy1 galaxies show variability in their CRTS long-term light curves on timescales larger than a day. The sources that showed variability on

Table 2
Correlation of Amplitude of Variability (σ_d) with Different Parameters, as in Table 1

Sample	redshift	Size	FWHM(Hβ)	R_{5007}	R_{4570}	$\log M_{\rm BH}/M_{\odot}$	$\log \lambda L_{5100}$	$\log \lambda_{\rm Edd}$
NLSy1	0.0–0.2	270	−0.03(5e−01)	−0.11(5e−02)	−0.17(4e−03)	0.04(5e−01)	0.09(1e−01)	0.07(2e−01)
BLSy1		367	0.03(5e−01)	−0.11(2e−02)	−0.17(1e−03)	0.07(1e−01)	0.14(4e−03)	0.01(8e−01)
All		637	0.01(8e−01)	−0.11(2e−03)	−0.16(3e−05)	0.04(3e−01)	0.11(4e−03)	0.01(6e−01)
NLSy1	0.2–0.4	685	0.07(4e−02)	−0.03(4e−01)	−0.23(2e−09)	0.12(7e−04)	0.08(2e−02)	−0.01(8e−01)
BLSy1		863	0.19(1e−08)	−0.08(1e−02)	−0.19(1e−08)	0.21(1e−10)	0.11(5e−04)	−0.16(2e−06)
All		1548	0.21(4e−18)	−0.06(8e−03)	−0.25(1e−23)	0.23(6e−21)	0.13(1e−07)	−0.18(1e−13)
NLSy1	0.4–0.6	612	0.09(1e−01)	0.00(9e−01)	−0.24(1e−09)	−0.10(1e−02)	−0.30(1e−14)	−0.27(3e−12)
BLSy1		847	0.20(3e−09)	0.06(4e−02)	−0.39(3e−31)	0.12(4e−04)	−0.27(4e−16)	−0.25(2e−14)
All		1459	0.28(2e−28)	0.03(1e−01)	−0.38(2e−51)	0.21(1e−16)	−0.17(8e−11)	−0.34(6e−42)
NLSy1	0.6–0.8	571	−0.00(9e−01)	0.09(1e−02)	−0.29(8e−13)	−0.35(4e−18)	−0.49(2e−36)	−0.33(1e−16)
BLSy1		841	0.23(2e−12)	0.10(2e−03)	−0.34(1e−24)	0.11(6e−03)	−0.42(7e−39)	−0.32(1e−22)
All		1412	0.27(3e−25)	0.09(6e−04)	−0.37(3e−48)	0.16(2e−10)	−0.32(4e−35)	−0.37(2e−49)

Note. The values given in columns 4–9 are the Spearman correlation coefficients (the p-value of no correlation).

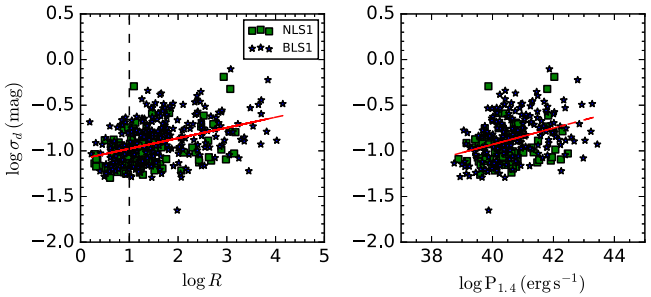

Figure 11. The σ_d vs. radio-loudness (left) and radio-power (right) is plotted. The dashed line at $\log R = 1$ in the left panel is the dividing line between radio-loud and radio-quiet objects. The solid lines represent the best linear fit to the relation. Spearman rank correlation coefficients (p-value) are 0.40 (2×10^{-17}) for the $\sigma_d - R$ relation and 0.36 (8×10^{-11}) for the $\sigma_d - P_{1.4}$ relation, respectively, considering the total sample.

timescales larger than a day are further considered for detailed analysis. Our main findings are as follows.

1. The median amplitude of variability is found to be $0.107^{+0.057}_{-0.032}$ mag for NLSy1 galaxies and $0.129^{+0.082}_{-0.049}$ for BLSy1 galaxies. Though the median values of σ_d agree within the error bars, a K–S test confirms with high significance that the two distributions are indeed different. Thus, NLSy1 galaxies as a class show a lower amplitude of variation in the optical than that seen in BLSy1 galaxies. However, in a subsample of NLSy1 and BLSy1 galaxies that have nearly identical $\lambda_{\rm Edd}$, the distribution of σ_d is found to be similar. Therefore, the larger amplitude of OV seen in BLSy1 galaxies relative to NLSy1 galaxies is due to them having a lower $\lambda_{\rm Edd}$ than NLSy1 galaxies.
2. Radio-loud objects in our sample in general are found to be more variable than their radio-quiet counterparts. Also, radio-loud BLSy1 galaxies are more variable than radio-loud NLSy1 galaxies, as confirmed by a K–S test. This increased variability in radio-loud sources both in NLSy1 and BLSy1 galaxies relative to radio-quiet sources might be due to the presence of non-thermal jet emission, in addition to the thermal disk emission within the galaxies, compared to the contribution of only thermal emission from the accretion disk to the optical light in radio-quiet sources.
3. When X-ray-detected NLSy1 and BLSy1 galaxies are considered separately, we find median amplitudes of variation of $0.099^{+0.043}_{-0.027}$ mag for XL-NLSy1 and $0.124^{+0.084}_{-0.047}$ mag for XL-BLSy1 galaxies. According to a K–S test, XL-BLSy1 galaxies are more variable than XL-NLSy1 galaxies.
4. A strong anti-correlation is found between the amplitude of variability and R_{4570} and $\lambda_{\rm EDD}$, suggesting the accretion disk as the main driver of the OV in both broad-line and narrow-line Seyfert 1 galaxies.
5. The amplitude of OV is found to be correlated with radio-loudness and radio-power. This hints at the contribution of jets in the OV of RL-NLSy1 and RL-BLSy1 galaxies in addition to the Eddington ratio, which is the main factor of OV in their radio-quiet counterparts.

We are grateful for the comments and suggestions by the anonymous referee, which helped to improve the manuscript. We thank Ying Zu for useful discussions on the JAVELIN code. S.R. thanks Neha Sharma for carefully reading this manuscript.

References

Ai, Y. L., Yuan, W., Zhou, H., et al. 2013, AJ, 145, 90
Ai, Y. L., Yuan, W., Zhou, H. Y., et al. 2010, ApJL, 716, L31
Alam, S., Albareti, F. D., Allende Prieto, C., et al. 2015, ApJS, 219, 12
Andrae, R., Kim, D.-W., & Bailer-Jones, C. A. L. 2013, A&A, 554, A137
Aretxaga, I., Cid Fernandes, R., & Terlevich, R. J. 1997, MNRAS, 286, 271
Baldi, R. D., Capetti, A., Robinson, A., Laor, A., & Behar, E. 2016, MNRAS, 458, L69
Bauer, A., Baltay, C., Coppi, P., et al. 2009, ApJ, 696, 1241
Becker, R. H., White, R. L., & Helfand, D. J. 1995, ApJ, 450, 559
Boller, T., Freyberg, M. J., Trümper, J., et al. 2016, A&A, 588, A103
Calderone, G., Ghisellini, G., Colpi, M., & Dotti, M. 2013, MNRAS, 431, 210
Cid Fernandes, R., Jr., Aretxaga, I., & Terlevich, R. 1996, MNRAS, 282, 1191
Cid Fernandes, R., Sodré, L., Jr., & Vieira da Silva, L., Jr. 2000, ApJ, 544, 123
Decarli, R., Dotti, M., Fontana, M., & Haardt, F. 2008, MNRAS, 386, L15
di Clemente, A., Giallongo, E., Natali, G., Trevese, D., & Vagnetti, F. 1996, ApJ, 463, 466
Doroshenko, V. T., Sergeev, S. G., Gaskell, C. M., et al. 2006, ARep, 50, 708
Drake, A. J., Catelan, M., Djorgovski, S. G., et al. 2013, ApJ, 763, 32
Drake, A. J., Djorgovski, S. G., Mahabal, A., et al. 2009, ApJ, 696, 870
Goodrich, R. W. 1989, ApJ, 342, 224
Graham, M. J., Djorgovski, S. G., Stern, D., et al. 2015, MNRAS, 453, 1562
Greenstein, J. L. 1963, Natur, 197, 1041
Grier, C. J., Peterson, B. M., Pogge, R. W., et al. 2012, ApJL, 744, L4
Grupe, D. 2004, AJ, 127, 1799
Hawkins, M. R. S. 2000, A&AS, 143, 465

Hook, I. M., McMahon, R. G., Boyle, B. J., & Irwin, M. J. 1994, MNRAS, 268, 305
Kaspi, S., Smith, P. S., Netzer, H., et al. 2000, ApJ, 533, 631
Kawaguchi, T., Mineshige, S., Umemura, M., & Turner, E. L. 1998, ApJ, 504, 671
Kellermann, K. I., Sramek, R., Schmidt, M., Shaffer, D. B., & Green, R. 1989, AJ, 98, 1195
Kelly, B. C., Bechtold, J., & Siemiginowska, A. 2009, ApJ, 698, 895
Klimek, E. S., Gaskell, C. M., & Hedrick, C. H. 2004, ApJ, 609, 69
Kozłowski, S. 2016a, MNRAS, 459, 2787
Kozłowski, S. 2016b, arXiv:1611.08248
Kozłowski, S. 2016c, ApJ, 826, 118
Kozłowski, S., Kochanek, C. S., Udalski, A., et al. 2010, ApJ, 708, 927
Leighly, K. M. 1999a, ApJS, 125, 297
Leighly, K. M. 1999b, ApJS, 125, 317
Li, S.-L., & Cao, X. 2008, MNRAS, 387, L41
Liu, X., Yang, P., Supriyanto, R., & Zhang, Z. 2016, IJAA, 6, 166
Lynden-Bell, D. 1969, Natur, 223, 690
MacLeod, C. L., Ivezić, Ž, Kochanek, C. S., et al. 2010, ApJ, 721, 1014
Meusinger, H., Hinze, A., & de Hoon, A. 2011, A&A, 525, A37
Miller, H. R., Ferrara, E. C., McFarland, J. P., et al. 2000, NewAR, 44, 539
Osterbrock, D. E., & Pogge, R. W. 1985, ApJ, 297, 166
Pancoast, A., Brewer, B. J., Treu, T., et al. 2014, MNRAS, 445, 3073
Press, W. H., Teukolsky, S. A., Vetterling, W. T., & Flannery, B. P. 1992, Numerical recipes in FORTRAN. The Art of Scientific Computing (Cambridge: Cambridge Univ. Press)
Rakshit, S., Petrov, R. G., Meilland, A., & Hönig, S. F. 2015, MNRAS, 447, 2420
Rakshit, S., Stalin, C. S., Chand, H., & Zhang, X.-G. 2017, ApJS, 229, 39
Rees, M. J. 1984, ARA&A, 22, 471
Richards, G. T., Fan, X., Newberg, H. J., et al. 2002, AJ, 123, 2945
Schmidt, M. 1963, Natur, 197, 1040
Sesar, B., Ivezić, Ž, Lupton, R. H., et al. 2007, AJ, 134, 2236
Shakura, N. I., & Sunyaev, R. A. 1973, A&A, 24, 337
Ulrich, M.-H., Maraschi, L., & Urry, C. M. 1997, ARA&A, 35, 445
Vanden Berk, D. E., Wilhite, B. C., Kron, R. G., et al. 2004, ApJ, 601, 692
Véron-Cetty, M.-P., Véron, P., & Gonçalves, A. C. 2001, A&A, 372, 730
Wagner, S. J., & Witzel, A. 1995, ARA&A, 33, 163
Wilhite, B. C., Brunner, R. J., Grier, C. J., Schneider, D. P., & Vanden Berk, D. E. 2008, MNRAS, 383, 1232
Wold, M., Brotherton, M. S., & Shang, Z. 2007, MNRAS, 375, 989
Woo, J.-H., & Urry, C. M. 2002, ApJ, 579, 530
Xu, D., Komossa, S., Zhou, H., et al. 2012, AJ, 143, 83
Young, A. J., Crawford, C. S., Fabian, A. C., Brandt, W. N., & O'Brien, P. T. 1999, MNRAS, 304, L46
Zhou, H., Wang, T., Yuan, W., et al. 2006, ApJS, 166, 128
Zu, Y., Kochanek, C. S., Kozłowski, S., & Peterson, B. M. 2016, ApJ, 819, 122
Zu, Y., Kochanek, C. S., Kozłowski, S., & Udalski, A. 2013, ApJ, 765, 106
Zu, Y., Kochanek, C. S., & Peterson, B. M. 2011, ApJ, 735, 80